

A kinetic study of catalytic methanol decomposition over nickel supported on silica

Yasuyuki Matsumura*† and Naoki Tode

Osaka National Research Institute, AIST, Midorigaoka, Ikeda, Osaka 563-8577, Japan

Received 3rd November 2000, Accepted 1st February 2001

First published as an Advance Article on the web 13th March 2001

A kinetic study of catalytic methanol decomposition to carbon monoxide and hydrogen over nickel supported on silica has been carried out with a flow reaction system in the temperature range of 433–498 K. The active site probably consists of a pair of nickel atoms which can strongly adsorb hydrogen and carbon monoxide. The reaction pathway is assumed to be: (1) dissociative adsorption of methanol to methoxy groups and hydrogen adsorbed on nickel sites; (2) decomposition of the methoxy groups to adsorbed carbon monoxide and hydrogen; and (3) desorption of the surface carbon monoxide and hydrogen species. In the second process, which is the rate determining step, the surface hydrogen species promote the decomposition of the methoxy groups, but this contradicts previous studies of decomposition over a clean nickel surface on which hydrogen atoms in the methoxy groups probably transfer to free nickel sites. The kinetic analysis shows that almost all the active sites are occupied by adsorption species and the number of free nickel sites is very small under the chosen reaction conditions. Thus, the transfer of hydrogen to free sites will be a minor step, although this process should be energetically advantageous to the decomposition step in which the methoxy groups and the adsorbed hydrogen atoms interact.

Introduction

Methanol decomposition to carbon monoxide and hydrogen is endothermic, and the reaction is applicable to a methanol-fueled automobile in which the heat of the exhaust gas is recovered with the decomposition and the product gas is fed to the engine.¹ In practical application methanol decomposition is an on-site source of hydrogen and/or carbon monoxide for chemical processes and also for fuel cells. Catalysts containing nickel are generally active in methanol decomposition.^{2–24} In the development of a decomposition catalyst containing nickel, which is an inexpensive metal, the clarification of the active sites and the reaction mechanism is indispensable. In the case of nickel supported on silica the catalytic activity does not relate to the metallic surface area of nickel but to the amounts of carbon monoxide and hydrogen strongly adsorbed on the surface at room temperature.²⁴ Since the strong adsorption of carbon monoxide takes place on a well-crystallized nickel surface,²⁵ the relation between adsorption and activity suggests that the major active sites are present on the ordered metallic surface.²⁴ The reaction kinetics was studied with metallic nickel, such as nickel wire and Raney nickel, and it was proposed that hydrogen adsorbed on the surface promotes the cleavage of the C–H bond in the methoxy group which is formed by the dissociative adsorption of methanol.^{2,11} However, surface science studies showed no such interaction between the hydrogen atom and the methoxy group, and rather suggested the self-decomposition of the methoxy to carbon monoxide and hydrogen on the surface.^{26–28}

In this work we have studied the kinetics of methanol decomposition over nickel supported on silica to solve the

contradiction between the reaction kinetics and the findings of surface science.

Experimental

Nickel supported on silica was prepared by hydrolysis and polymerization of tetraethyl orthosilicate (GR grade, Kanto Chemical Co. Ltd) whose solution contained nickel nitrate [$\text{Ni}(\text{NO}_3)_2 \cdot 6\text{H}_2\text{O}$, GR, Kanto] and ethanol. After drying in air at 393 K the solid was heated in air for 5 h at 673 K for removal of NO_3^- anions and residual organic compounds. The sample contained 40 wt.% of nickel as metal (40 wt.% Ni–S). Nickel supported on commercial silica (Fuji-Silicia, ID-G) was prepared by impregnation with nickel nitrate. After the impregnation the solid was heated in air at 773 K for 5 h (10 wt.% Ni–I).

Adsorption of hydrogen was carried out in a vacuum system equipped with Baratron pressure gauges at room temperature. Just before the adsorption, a fresh sample was reduced with hydrogen (*ca.* 20 kPa) at 773 K for 1 h and evacuated at the same temperature for 0.5 h.

The BET surface areas of the catalysts were determined by the isotherms of nitrogen physisorption.

The catalytic experiments were performed in a fixed-bed continuous flow reactor operated at atmospheric pressure. The catalyst (0.05–0.40 g) was mixed with the commercial silica (total mass, 0.50 g) and sandwiched with quartz wool plugs in a tube reactor made of quartz glass (id 6 mm). It was confirmed that neither silica nor the reactor contributed to the reaction. After reducing the sample in a flow of hydrogen (20 vol.%) in argon for 1 h at 773 K, methanol was fed with an argon carrier at 433–498 K. Since carbon monoxide and hydrogen significantly affect the reaction rate, the gases were often co-fed in order to change the reaction composition. The total flow rate of the reaction gas was 1.8–7.5 $\text{dm}^3 \text{h}^{-1}$. The reactant and products were analyzed with an on-stream

† Present address: Research Institute of Innovative Technology for the Earth, Kizu-cho, Soraku-gun, Kyoto 619-0292, Japan. E-mail: yasuyuki@rite.or.jp

Table 1 Adsorption study of Ni/SiO₂

Sample	Amount of H ₂ adsorbed /μmol g(cat) ⁻¹		Surface area of Ni /m ² g(cat) ⁻¹	BET surface area /m ² g ⁻¹
	Strong ^a	At 20 kPa		
40 wt.% Ni-S	52	125	9.5	377
10 wt.% Ni-I	8	51	3.9	215

^a The amount adsorbed at a pressure less than 0.01 kPa.

Yanaco G2800 gas chromatograph (Porapak T, 4 m; Ar carrier) equipped with a thermal conductivity detector. The methanol conversion was always kept less than 10% and the partial pressures of the components employed here were the averages at the inlet and outlet of the reactor.

Results

Adsorption study of the catalysts

Adsorption of hydrogen was carried out at room temperature with the samples reduced at 773 K for 1 h. The surface area of

nickel was determined from the amount of hydrogen adsorbed at 20 kPa (Table 1) assuming stoichiometric adsorption of a hydrogen atom on a single nickel site, the atomic cross section of which is 0.0633 nm² (ref. 29). The amount of hydrogen adsorbed on 10 wt.% Ni-I at a pressure below 0.01 kPa was significantly smaller than that for 40 wt.% Ni-S (see Table 1).

The BET surface areas of 40 wt.% Ni-S and 10 wt.% Ni-I were 377 and 215 m² g⁻¹, respectively.

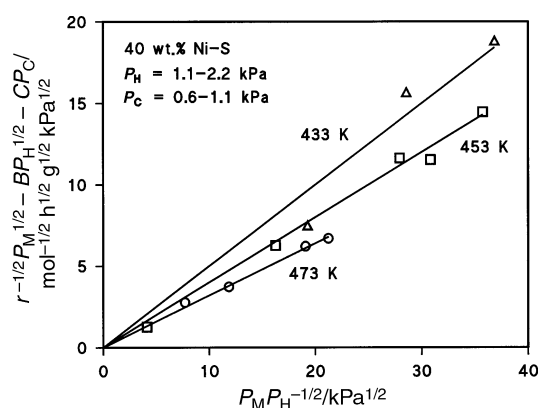


Fig. 1 Plot of $r^{-1/2}P_M^{1/2} - BP_H^{1/2} - CP_C$ vs. $P_M P_H^{-1/2}$ for methanol decomposition over 40 wt.% Ni-S.

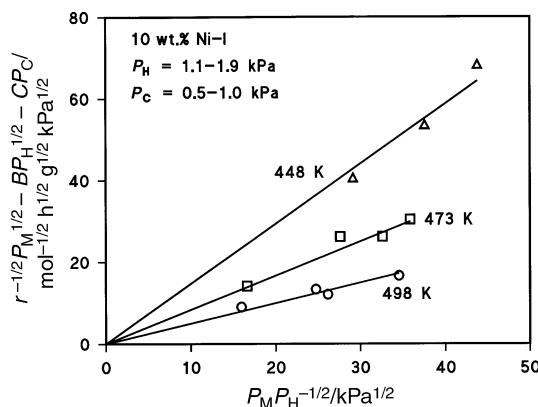


Fig. 2 Plot of $r^{-1/2}P_M^{1/2} - BP_H^{1/2} - CP_C$ vs. $P_M P_H^{-1/2}$ for methanol decomposition over 10 wt.% Ni-I.

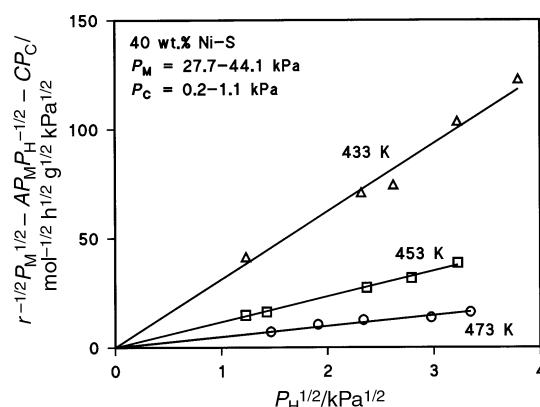


Fig. 3 Plot of $r^{-1/2}P_M^{1/2} - AP_M P_H^{-1/2} - CP_C$ vs. $P_H^{1/2}$ for methanol decomposition over 40 wt.% Ni-S.

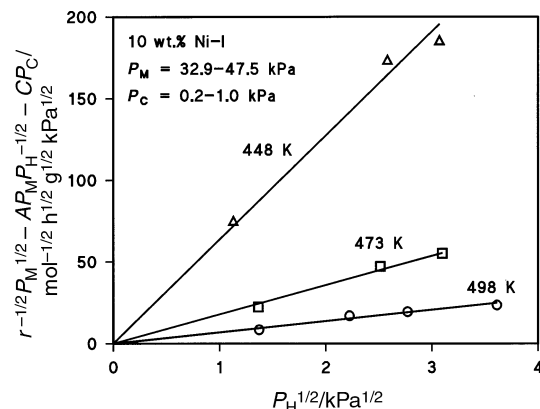


Fig. 4 Plot of $r^{-1/2}P_M^{1/2} - AP_M P_H^{-1/2} - CP_C$ vs. $P_H^{1/2}$ for methanol decomposition over 10 wt.% Ni-I.

Table 2 Rate constants of methanol decomposition over Ni/SiO₂

Catalyst	Temperature /K	A /mol ^{-1/2} h ^{1/2} g ^{1/2}	B /mol ^{-1/2} h ^{1/2} g ^{1/2}	C /mol ^{-1/2} h ^{1/2} g ^{1/2} kPa ^{-1/2}
40 wt.% Ni-S	473	0.32	4.9	0.66
	453	0.40	11.7	1.73
	433	0.50	31.2	8.27
10 wt.% Ni-I	498	0.50	6.9	0.77
	473	0.86	17.9	2.44
	448	1.47	63.7	15.7

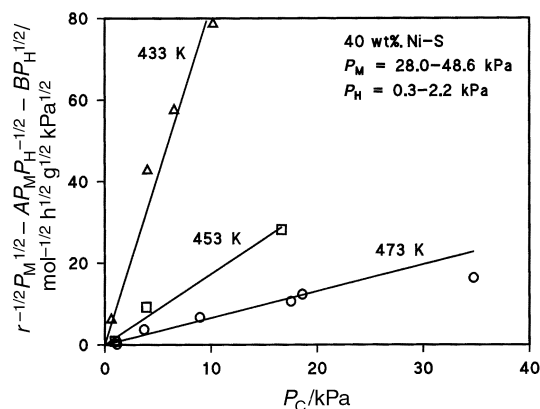


Fig. 5 Plot of $r^{-1/2}P_M^{1/2} - AP_M P_H^{-1/2} - BP_H^{1/2}$ vs. P_C for methanol decomposition over 40 wt.% Ni-S.

Reaction kinetics

Methanol was stoichiometrically decomposed to carbon monoxide and hydrogen over the nickel catalysts under the chosen reaction conditions. Negligible amounts of methane and water were detected as by-products. The kinetic data can be fitted with the following equation, which is derived from the reaction kinetics described in the Discussion section:

$$r^{-1/2}P_M^{1/2} = AP_M P_H^{-1/2} + BP_H^{1/2} + CP_C \quad (I)$$

where r is the rate of carbon monoxide formation, and P_M , P_H and P_C are the partial pressures of methanol, hydrogen and carbon monoxide, respectively. The constants, A , B and C , are listed in Table 2. Figs. 1 and 2 show the plots of $r^{-1/2}P_M^{1/2} - BP_H^{1/2} - CP_C$ vs. $P_M P_H^{-1/2}$ for the two catalysts, and the value A is the slope of the line. Figs. 3 and 4 and Figs. 5 and 6 show the plots of $r^{-1/2}P_M^{1/2} - AP_M P_H^{-1/2} - CP_C$ vs. $P_H^{1/2}$ and the plots of $r^{-1/2}P_M^{1/2} - AP_M P_H^{-1/2} - BP_H^{1/2}$ vs. P_C , respectively. The values B and C are the slopes of the respective lines.

Discussion

Yasumori *et al.*² proposed the following reaction mechanism for methanol decomposition over a nickel surface:

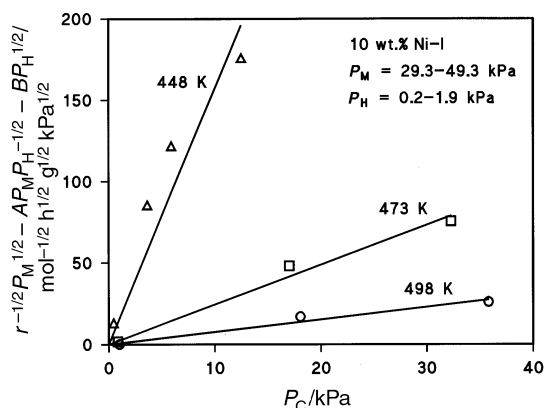
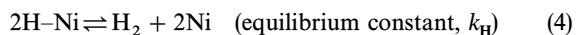
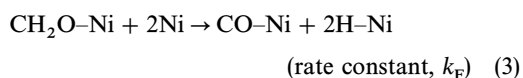
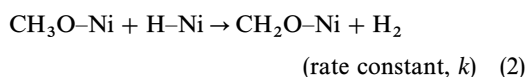
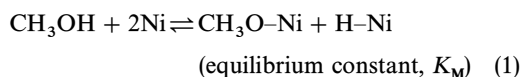
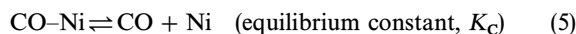


Fig. 6 Plot of $r^{-1/2}P_M^{1/2} - AP_M P_H^{-1/2} - BP_H^{1/2}$ vs. P_C for methanol decomposition over 10 wt.% Ni-I.



The dissociative adsorption of methanol to methoxy groups (step 1) and the adsorption of hydrogen and carbon monoxide (steps 4 and 5) can take place on the surface of nickel metal.²⁵⁻²⁷ When step 2 is the rate determining step and the reaction is at steady state, the following equations can be derived:

$$\theta_H = K_H^{-1/2} P_H^{1/2} \theta_S \quad (6)$$

$$\theta_C = K_C^{-1} P_C \theta_S \quad (7)$$

$$\theta_M = K_M P_M \theta_H^{-1} \theta_S^2 = K_M K_H^{1/2} P_M P_H^{-1/2} \theta_S \quad (8)$$

where θ_S , θ_H , θ_C , and θ_M are the fractions of Ni (free nickel site), H-Ni, CO-Ni and CH₃O-Ni, respectively, and

$$1 = \theta_M + \theta_H + \theta_C + \theta_S \quad (9)$$

Thus,

$$\theta_S = (K_M K_H^{1/2} P_M P_H^{-1/2} + K_H^{-1/2} P_H^{1/2} + K_C^{-1} P_C + 1)^{-1} \quad (10)$$

Since step 2 is rate determining,

$$\begin{aligned} r &= k \theta_M \theta_H = k K_M P_M \theta_S^2 \\ &= k K_M P_M (K_M K_H^{1/2} P_M P_H^{-1/2} + K_H^{-1/2} P_H^{1/2} + K_C^{-1} P_C + 1)^{-2} \end{aligned} \quad (11)$$

The rates of formation and decomposition of CH₂O-Ni (steps 2 and 3) should be balanced, thus

$$r = k_F \theta_F \theta_S^2 \quad (12)$$

where θ_F is the fraction of CH₂O-Ni. From eqns. (11) and (12)

$$\theta_F = k K_M P_M k_F^{-1} \quad (13)$$

is obtained. Since the decomposition of formaldehyde (step 3) occurs easily on nickel catalysts,^{2,5} k_F is considered to be much larger than k . Hence, θ_F can be negligible and step 3 does not contribute to the equation. Then eqn. (11) can be transformed to

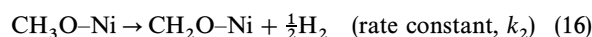
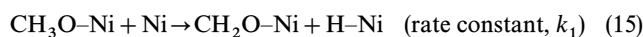
$$\begin{aligned} r^{-1/2} P_M^{1/2} &= k^{-1/2} K_M^{1/2} K_H^{1/2} P_M P_H^{-1/2} + k^{-1/2} K_M^{-1/2} K_H^{-1/2} P_H^{1/2} \\ &\quad + k^{-1/2} K_M^{-1/2} K_C^{-1} P_C + k^{-1/2} K_M^{-1/2} \end{aligned} \quad (14)$$

When the $k^{-1/2} K_M^{-1/2}$ term is negligible, the equation can be expressed as

$$\begin{aligned} r^{-1/2} P_M^{1/2} &= k^{-1/2} K_M^{1/2} K_H^{1/2} P_M P_H^{-1/2} \\ &\quad + k^{-1/2} K_M^{-1/2} K_H^{-1/2} P_H^{1/2} \\ &\quad + k^{-1/2} K_M^{-1/2} K_C^{-1} P_C \end{aligned} \quad (II)$$

This rate equation is consistent with the experimental one [eqn. (I)].

We derived other rate equations assuming the rate determining steps to be



The following rate equations can be obtained at steady state:

$$\begin{aligned} r^{-1/2} P_M^{1/2} P_H^{-1/4} &= k_1^{-1/2} K_M^{1/2} P_M P_H^{-1/2} + k_1^{-1/2} K_M^{-1/2} K_H^{-3/4} P_H^{1/2} \\ &\quad + k_1^{-1/2} K_M^{-1/2} K_H^{-1/4} K_C^{-1} P_C + k_1^{-1/2} K_M^{-1/2} K_H^{-1/4} \end{aligned} \quad (17)$$

$$\begin{aligned} r^{-1/2} P_M P_H^{-1/2} &= k_2^{-1} P_M P_H^{-1/2} + k_2^{-1} K_M^{-1} K_H^{-1} P_H^{1/2} \\ &\quad + k_2^{-1} K_M^{-1} K_H^{-1/2} K_C^{-1} P_C + k_2^{-1} K_M^{-1} K_H^{-1/2} \end{aligned} \quad (18)$$

respectively. However, no linear relationship was obtained on the basis of the rate expressions; hence, the mechanisms (15) and (16) are less probable.

The three kinetic parameters k , $K_M K_H$ and $K_H^{-1/2} K_C$ can be obtained as $A^{-1} B^{-1}$, AB^{-1} and BC^{-1} , respectively, by comparison between eqns. (I) and (II). These parameters at 473 K are listed in Table 3. The activation energy of step 2 (E_a) and the heats of adsorption of methanol, hydrogen and carbon monoxide (Q_M , Q_H and Q_C , respectively) are related to r , K_M , K_H and K_C as follows:

$$r = A e^{-E_a/RT} \quad (19)$$

$$K_M = A_M e^{Q_M/RT} \quad (20)$$

$$K_H = A_H e^{-Q_H/RT} \quad (21)$$

$$K_C = A_C e^{-Q_C/RT} \quad (22)$$

where A , A_M , A_H and A_C are frequency factors. Thus, the values of E_a , $Q_H - Q_M$ and $Q_C - 0.5Q_H$ were calculated from the Arrhenius plots of k , $K_M K_H$ and $K_H^{-1/2} K_C$ (Table 4 and Fig. 7).

The activity of Ni/SiO₂ relates empirically to the amount of hydrogen or carbon monoxide strongly adsorbed.²⁴ Thus, the active site is considered to adsorb hydrogen strongly. The activation energy for hydrogen desorption from a nickel surface was reported^{26,27,30} to be 90–117 kJ mol⁻¹. Assuming that the value is the same as the heat of adsorption of hydrogen, the heats of adsorption of methanol can be calculated as 30–57 and 48–75 kJ mol⁻¹ for 40 wt.% Ni-S and 10 wt.% Ni-I, respectively. The activation energy of methanol desorption from the nickel surface was reported^{26–28} to be 41–67 kJ mol⁻¹, and the value is close to the heat of adsorption of methanol calculated here (see Table 4). On the other hand, the

Table 3 Kinetic parameters at 473 K

Catalyst	k /mol h ⁻¹ g ⁻¹	$K_M K_H$	$K_H^{-1/2} K_C$ /kPa ^{1/2}
40 wt.% Ni-S	0.64	0.065	7.5
10 wt.% Ni-I	0.05	0.065	7.3

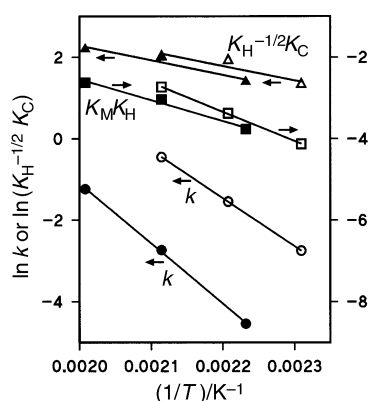


Fig. 7 Arrhenius plot of the rate constants. Open symbols, 40 wt.% Ni-S; solid symbols, 10 wt.% Ni-I.

Table 4 The activation energy and the heats of adsorption

Catalyst	E_a /kJ mol ⁻¹	$Q_H - Q_M$ /kJ mol ⁻¹	$Q_C - 0.5Q_H$ /kJ mol ⁻¹	Q_H /kJ mol ⁻¹	Q_M /kJ mol ⁻¹	Q_C /kJ mol ⁻¹
40 wt.% Ni-S	98	60	29		30–57 ^a	74–88 ^a
10 wt.% Ni-I	123	42	30		48–75 ^a	75–89 ^a
Ni surface ^b	67			90–117	41–67	130

^a The values are calculated on the assumption of $Q_H = 90$ –117 kJ mol⁻¹. ^b The values are taken from refs. 26–28, 30 and 31.

heat of adsorption of carbon monoxide can be estimated as 74–89 kJ mol⁻¹. The activation energy of carbon monoxide desorption from a nickel surface was reported^{26,27,31} to be ca. 130 kJ mol⁻¹, and the values obtained were lower than that. In step 5 carbon monoxide desorbs from a single nickel site. However, actual adsorption of carbon monoxide on nickel is not so simple. At room temperature two adsorption species, *i.e.*, bridge and linear, are known for strongly adsorbed carbon monoxide,^{25,32,33} but the fraction of the bridge species decreases with increasing coverage of carbon monoxide and increasing temperature.^{34,35} Under the chosen reaction conditions the temperature is so high that the bridge species will be minor. On the surface hydrogen is co-adsorbed. Since the ratio of the fractions of H-Ni and CO-Ni relates to the value of $K_H^{-1/2} K_C$, *i.e.*, $\theta_H \theta_C^{-1} = K_H^{-1/2} K_C P_H^{1/2} P_C^{-1}$, the coverage of hydrogen on the surface is usually higher than that of carbon monoxide under the chosen reaction conditions. This suggests that the presence of hydrogen atoms on the surface disturbs the adsorption of carbon monoxide and, as a result, the adsorption strength will be weaker.

When the fraction of free nickel surface sites is small ($\theta_s \ll 1$), the term $k^{-1/2} K_M^{-1/2}$ in eqn. (16) will be negligible. Hence, the absence of the term $k^{-1/2} K_M^{-1/2}$ in eqn. (II) implies that the surface sites are almost entirely covered with the adsorption species. On the basis of the rate equation [eqn. (II)], we simulated the changes in reaction rate and surface fractions of CH₃O-Ni, H-Ni and CO-Ni with changes in the composition of the reaction mixture when 50 kPa of methanol is initially supplied with argon over 40 wt.% Ni-S at 473 K under atmospheric pressure (Fig. 8). In the figure the change in the composition is expressed by the conversion of methanol. It is noteworthy that the rate increases with methanol conversion in the low conversion range. At low methanol conversion where the partial pressure of hydrogen is low, the fraction of H-Ni increases drastically with increase in methanol conversion because the rate relates to the surface fractions of both CH₃O-Ni and H-Ni (step 2). Yasumori *et al.*² confirmed the promotional effect of hydrogen in methanol decomposition over nickel wire with a circulation system operated below 3 kPa, while we were unable to obtain kinetic data at a very small contact time with the flow reaction system. On the other

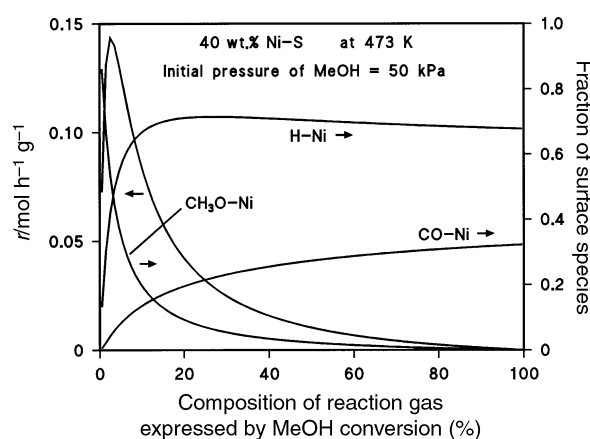


Fig. 8 Relationship between the reaction gas composition and the reaction rate for 40 wt.% Ni-S at 473 K.

hand, the study of methanol decomposition on a clean nickel surface shows hydrogen transfer from the methoxy species to the surface of nickel such as by mechanism (15). The activation energy of the decomposition of the methoxy group on a clean nickel surface was reported²⁸ to be 67 kJ mol⁻¹, and this reaction step is probably advantageous to step 2, the activation energy of which is considerably larger than that (see Table 4). However, under the conditions of the flow reaction, the pressure of methanol is so high that the surface fraction of free nickel sites is negligibly small. Hence, the probability of reaction (15) is actually small, and reaction mainly takes place between CH₃O–Ni and H–Ni, although the step is energetically less advantageous. This reaction mechanism suggests that the active site comprises two nickel sites.

The kinetic parameters for 10 wt.% Ni–I are similar to those for 40 wt.% Ni–S except for the values of *k* (see Fig. 7). The rate constant, *k*, relates to the number of active sites, and the number of sites strongly adsorbing hydrogen on 10 wt.% Ni–I is significantly smaller than on 40 wt.% Ni–S. Hence, the difference in the constant, *k*, is mainly due to the difference in the quantity of active sites that can strongly adsorb hydrogen, while the quality of the sites for 10 wt.% Ni–I is similar to that for 40 wt.% Ni–S.

Conclusions

The reaction kinetics of the decomposition of methanol to hydrogen and carbon monoxide below 500 K over nickel supported on silica can be expressed as

$$r^{-1/2}P_M^{1/2} = AP_M P_H^{-1/2} + BP_H^{1/2} + CP_C,$$

where *r* is the rate of carbon monoxide formation, and *P_M*, *P_H* and *P_C* are the partial pressures of methanol, hydrogen and carbon monoxide, respectively. The equation is consistent with the rate derived from the following reaction steps: (1) dissociative adsorption of methanol to methoxy groups and hydrogen adsorbed on nickel sites (CH₃OH + 2Ni ⇌ CH₃O–Ni + H–Ni); (2) decomposition of the methoxy groups promoted by the adsorbed hydrogen (CH₃O–Ni + H–Ni → CH₂O–Ni + H₂ and CH₂O–Ni + 2Ni → CO–Ni + 2H–Ni); and (3) desorption of the surface carbon monoxide and hydrogen species (2H–Ni ⇌ H₂ + 2Ni and CO–Ni ⇌ CO + Ni). The heats of adsorption of methanol and carbon monoxide can be estimated on the assumption that the heat of adsorption of hydrogen is 90–117 kJ mol⁻¹. The heat of adsorption of methanol estimated is close to the activation energy for methanol desorption from a clean nickel surface. However, the heat of adsorption of carbon monoxide is significantly smaller than that estimated from the adsorption on a clean nickel surface, and it may be due to co-adsorption of hydrogen. The active site comprises two nickel atoms which are almost covered with adsorption species such as atomic hydrogen, carbon monoxide and methoxy groups. Thus, the decomposition of methoxy groups with free nickel sites (CH₃O–Ni + Ni → CH₂O–Ni + H–Ni), which can proceed on a clean nickel surface, is disadvantageous under the actual reaction conditions because of the lack of free nickel sites,

although the activation energy of the process on a clean surface is probably lower than that for the decomposition process promoted by adsorbed hydrogen.

References

- 1 National Research Council, *Catalysis Looks to the Future*, National Academy Press, Washington, DC, 1992.
- 2 I. Yasumori, T. Nakamura and E. Miyazaki, *Bull. Chem. Soc. Jpn.*, 1967, **40**, 1372.
- 3 I. Yasumori and E. Miyazaki, *Nippon Kagakukaishi*, 1971, **92**, 659.
- 4 S. Kasaoka and T. Shiraga, *Nenryo Kyokaishi*, 1980, **59**, 40.
- 5 H. Niiyama, S. Tamai, J.-S. Kim and E. Echigoya, *Sekiyu Gakkaishi*, 1981, **24**, 322.
- 6 A. Tada, T. Yoshino and H. Itoh, *Chem. Lett.*, 1987, 419.
- 7 M. Akiyoshi, H. Hattori and K. Tanabe, *Sekiyu Gakkaishi*, 1987, **30**, 156.
- 8 M. Shimizu, K. Nobori and S. Takeoka, *Kagaku Kogaku Ronbunshu*, 1988, **14**, 114.
- 9 M. Akiyoshi and H. Hattori, *Sekiyu Gakkaishi*, 1988, **31**, 239.
- 10 Y. Nakazaki and T. Inui, *Ind. Eng. Chem. Res.*, 1989, **28**, 1285.
- 11 M. Shimizu and S. Takeoka, *Kagaku Kogaku Ronbunshu*, 1989, **15**, 284.
- 12 O. Tokunaga, Y. Satoh, T. Fukushima and S. Ogasawara, *Sekiyu Gakkaishi*, 1990, **33**, 173.
- 13 H. Imai, T. Tagawa and K. Nakamura, *Appl. Catal.*, 1990, **62**, 348.
- 14 H. Imamura, T. Takada, S. Kasahara and S. Tsuchiya, *Appl. Catal.*, 1990, **58**, 165.
- 15 A. Tada, Y. Watarai, K. Takahashi, Y. Imizu and H. Itoh, *Chem. Lett.*, 1990, 543.
- 16 T. Okubo, M. Watanabe, K. Kusakabe and S. Morooka, *Key Eng. Mater.*, 1991, **61&62**, 71.
- 17 M. Morita, K. Takeda, S. Tanabe and Y. Matsuda, *Nippon Kagakukaishi*, 1991, 1238.
- 18 M. Watanabe, T. Okubo, K. Kusakabe and S. Morooka, *Ind. Eng. Chem. Res.*, 1992, **31**, 2633.
- 19 B. Chen and J. L. Falconer, *J. Catal.*, 1993, **144**, 214.
- 20 K. J. Yoon, K. S. Jeong and J. E. Yie, *Hwahak Konghak*, 1993, **31**, 569.
- 21 Y. Matsumura, N. Tode, T. Yazawa and M. Haruta, *J. Mol. Catal. A: Chem.*, 1995, **99**, 183.
- 22 Y. Matsumura, K. Kagawa, Y. Usami, M. Kawazoe, H. Sakurai and M. Haruta, *Chem. Commun.*, 1997, 657.
- 23 Y. Matsumura, K. Kuraoka, T. Yazawa and M. Haruta, *Catal. Today*, 1998, **45**, 191.
- 24 Y. Matsumura, K. Tanaka, N. Tode, T. Yazawa and M. Haruta, *J. Mol. Catal. A: Chem.*, 2000, **152**, 157.
- 25 J. T. Yates and C. W. Garland, *J. Phys. Chem.*, 1961, **65**, 617.
- 26 S. R. Bare, J. A. Stroschio and W. Ho, *Surf. Sci.*, 1985, **150**, 399.
- 27 L. J. Ritcher and W. Ho, *J. Chem. Phys.*, 1985, **83**, 2569.
- 28 J. J. Vajo, J. H. Campbell and H. B. Christopher, *J. Phys. Chem.*, 1991, **95**, 9457.
- 29 J. W. E. Coenen, *Appl. Catal.*, 1991, **75**, 193.
- 30 K. Christmann, O. Schober, G. Ertl and M. Neumann, *J. Chem. Phys.*, 1974, **60**, 4528.
- 31 N. Takagi, J. Yoshinobu and M. Kawai, *Chem. Phys. Lett.*, 1993, **215**, 120.
- 32 C. E. O'Neill and D. J. C. Yates, *J. Phys. Chem.*, 1961, **65**, 617.
- 33 M. Primet, J. A. Dalmon and G. A. Martin, *J. Catal.*, 1977, **46**, 25.
- 34 J. Lauterbach, M. Wittmann and J. Küppers, *Surf. Sci.*, 1992, **279**, 287.
- 35 J. Yoshinobu and M. Kawai, *Surf. Sci.*, 1996, **363**, 105.